Bicyclo-DNA: a Hoogsteen-selective pairing system

Martin Bolli, J Christopher Litten, Rolf Schütz and Christian J Leumann*

Background: The natural nucleic acids (DNA and RNA) can adopt a variety of structures besides the antiparallel double helix described by Watson and Crick, depending on base sequence and solvent conditions. Specifically base-paired DNA structures with regular backbone units include left-handed and parallel duplexes and triple and quadruple helical arrangements. Given the base-pairing pattern of the natural bases, preferences for how single strands associate are determined by the structure and flexibility of the sugar-phosphate backbone. We set out to determine the role of the backbone in complex formation by designing DNA analogs with well defined modifications in backbone structure.

Results: We recently developed a DNA analog (bicyclo-DNA) in which one (γ) of the six torsion angles (α–ζ) describing the DNA-backbone conformation is fixed in an orientation that deviates from that observed in B-DNA duplexes by about +100°, a shift from the synclinal to the antiperiplanar range. Upon duplex formation between homopurine and homopyrimidine sequences, this analog preferentially selects the Hoogsteen and reversed Hoogsteen mode, forming A–T and G–C$^+$ base pairs. Base-pair formation is highly selective, but degeneracy is observed with respect to strand orientation in the duplex.

Conclusions: The flexibility and orientation of the DNA backbone can influence the preferences of the natural bases for base-pairing modes, and can alter the relative stability of duplexes and triplexes.

Addresses: Institut für Organische Chemie, Universität Bern, Freiestrasse 3, CH-3012 Bern, Switzerland.

*Corresponding author.

Key words: backbone modification, 1-deazaadenine, DNA analog, DNA triple helix, Hoogsteen duplex

Received: **26 Feb 1996**
Revisions requested: **5 Mar 1996**
Revisions received: **11 Mar 1996**
Accepted: **11 Mar 1996**

Chemistry & Biology March 1996, **3**:197–206

Introduction

The selective supramolecular organization of the natural nucleic acids (DNA and RNA) into base-paired complexes is defined by the hydrogen-bonding pattern of the nucleobases and the structure of the sugar-phosphate backbone. The number of possible base–base interactions is large, and the conformation of the (deoxy)ribofuranose-phosphate backbone is relatively flexible, so that a multitude of different mono- and multi-stranded complexes can exist, depending on the base sequence, the chain length and the external conditions (such as pH, ionic strength, coordinating metal ions and solvent). Although the catalog of potential pairing motifs of DNA and RNA is still incomplete, a number of structural elements different from the well known right-handed antiparallel Watson–Crick double helix have been identified. Examples include left-handed Z-DNA [1], parallel duplexes with reversed Watson–Crick A–T [2–4], or Hoogsteen base pairs (A–T and G–C$^+$, where C$^+$ is protonated cytosine) [5,6], two different modes of triple helices [7–10], a pair of intertwined duplexes held together by C–C$^+$ base-pairs (the i-motif) [11,12] and a whole class of G-tetrad motifs [13–15].

This variety of possible structures raises the question of how much the structure and flexibility of the sugar-phosphate backbone influence the mode and selectivity of complex formation. This question can be experimentally addressed by synthesizing and analyzing oligonucleotide analogs with defined changes in their repeating backbone unit. To date, however, only a handful of DNA analogs have been sufficiently characterized to contribute to the answer to this question. Pioneering studies on homo-DNA, built from 4'→6'-linked 2',3'-dideoxy-β-D-glucopyranosyl nucleotides [16–19], showed that the backbone torsion angle δ was important for both structure and base-pairing properties.These results were placed into perspective with natural DNA and RNA structures. Recent work on *p*-RNA, a RNA isomer consisting of 2'→4'-linked β-D-ribopyranosyl nucleotides, shed further light into the topological factors determining the chain orientation and association mode in duplexes [20,21].

'Bicyclo-DNA' (Fig. 1) is a DNA analog that differs from natural DNA by an additional ethylene bridge located between the centers C(3') and C(5'). This change in the carbon skeleton of the original deoxyribose gives a locked sugar conformation in which the torsion angle δ (which is 120–140° in the 1'-*exo*, 2'-*endo* furanose conformation) is close to that of normal B-DNA, but the neighboring torsion angle γ is restricted to the antiperiplanar range (140–160°) [22,23] and thus deviates from that observed in natural A- or B-DNA by ~100°. Any change of the base-pairing properties of bicyclo-DNA relative to natural DNA can therefore be directly related to the structural change around the C(4')–C(5') bond in its repeating backbone

Figure 1

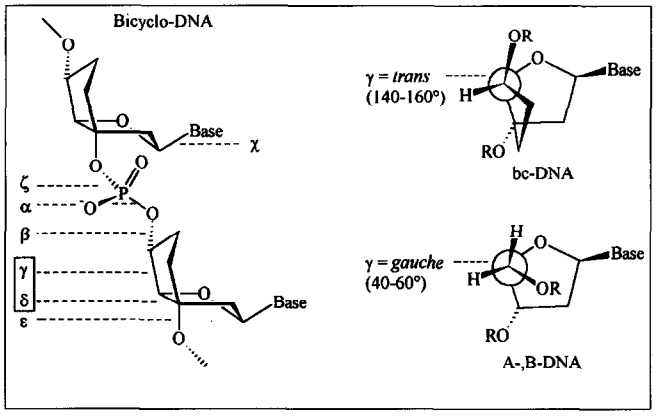

Structure and conformational preferences of bicyclo-DNA. The γ torsion angle for A- and B-DNA is shown for comparison.

Figure 2

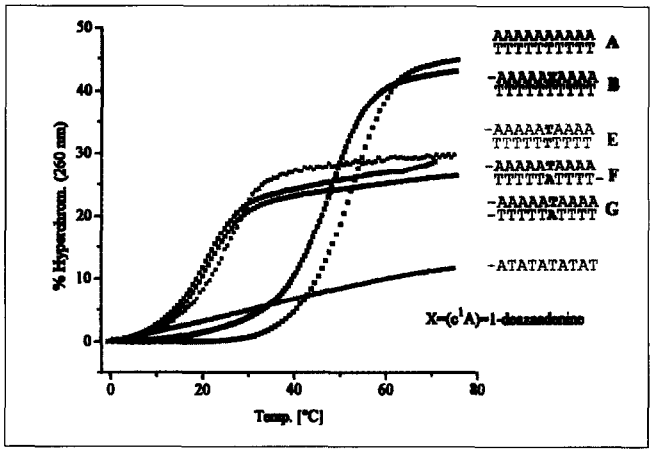

Conversion of an A–T to a T–A base pair in a bicyclo-DNA duplex causes dramatic changes in melting temperature. UV melting curves (λ = 260 nm) are shown for the bicyclo-oligonucleotide duplexes A,B,E,F and G (Table 1) and the single-stranded sequence bcd(AT)$_5$. In duplexes F and G, the central base pair for parallel or antiparallel strands has been changed from A–T to T–A; in both cases, the T_m is decreased to approximately the same T_m as a mismatched duplex (E). Insertion of the unnatural base 1-deazaadenine (purine strand in B) has little effect on T_m, whereas the self-complementary sequence bcd(AT)$_5$ appears to fail to form a duplex altogether. In asymmetrical sequences a hyphen denotes the 5'-end. Experimental conditions as for Table 1.

unit. The bicyclo-DNA sequences bcd(A_{10}) and bcd(T_{10}) were previously shown to form duplex and triplex structures that are more stable than those of the corresponding natural DNA [24]. Circular dichroism (CD) spectroscopy indicated that the double helical structure was different from that in the natural system, however [25]. Here we report that this duplex is of the Hoogsteen type and that the preference for Hoogsteen and reversed-Hoogsteen pairing over Watson–Crick duplex formation is a general structural property of bicyclo-DNA.

Results and discussion

Bicyclo-DNA sequences containing adenine and thymine. To determine the association mode in the duplex bcd(A_{10}).bcd(T_{10}), we performed the following experiments. First, we investigated the stability of a decamer duplex, in which the central A–T base pair was converted to a T–A base pair. This change is associated with a decrease in the melting temperature (T_m) of 30 °C, irrespective of whether the strands are parallel or antiparallel (Fig. 2, Table 1, F,G). This conversion destabilizes the duplex to the same degree as an A–A or a T–T mismatch at the same location (Table 1, C–E) and must thus also be considered a mismatch. An even more dramatic example of this behavior is the observation that the self-complementary alternating sequence bcd(AT)$_5$ completely fails to form a duplex (Fig. 2). These results are *a priori* incompatible with base pairing according to the Watson–Crick or reversed Watson–Crick modes, and suggest that the preferred association mode involves Hoogsteen or reversed Hoogsteen A–T base pairs (Fig. 3).

Bcd(T_{10}) and bcd(A_{10}) at the stoichiometric ratio 2:1 form a triplex with a classical biphasic UV-melting profile upon heat denaturation, as do the natural sequences d(T_{10}) and d(A_{10}) (Fig. 4a). For the d(A_{10}).2d(T_{10}) triplex it is known that the low-temperature melting event, ascribed to the loss of the T-strand bound to the Hoogsteen side of the purine strand, is observable at all wavelengths in the range of 250–290 nm, whereas the melting event at higher temperature, associated with the rupture of the Watson–Crick duplex to give free single strands, shows isosbestic behavior at 284 nm [26]. In the case of the analogous bicyclo-DNA system, similar UV-spectroscopic behavior was observed, with the important difference that the melting event at lower temperature is invisible at 284 nm. This is consistent with the notion that the Watson–Crick T-strand melts at lower

Table 1

T_m values for decameric bicyclonucleotide duplexes.

	Sequence	T_m (Conc.)
A	bcd(AAAAAAAAAA)/bcd(TTTTTTTTTT)	52.9 °C (3.3 μM)
B	bcd(AAAAA(c¹A)AAAA)/bcd(TTTTTTTTTT)	48.7 °C (4.2 μM)
C	bcd(AAAAAAAAAA)/bcd(TTTTATTTTT)	21.2 °C (4.2 μM)
D	bcd(AAAAAAAAAA)/bcd(TTTTTATTTT)	21.3 °C (4.4 μM)
E	bcd(AAAAATAAAA)/bcd(TTTTTTTTTT)	24.2 °C (4.9 μM)
F	bcd(AAAAATAAAA)/bcd(TTTTATTTTT)	21.0 °C (4.7 μM)
G	bcd(AAAAATAAAA)/bcd(TTTTTATTTT)	21.9 °C (4.9 μM)

Duplexes A–G contain homobasic or mixed sequences comprising the nucleobases adenine (A), thymine (T) and 1-deazaadenine (c¹A). Melting was studied at λ = 260 nm. Conc., concentration in 10 mM NaH_2PO_4, 1 M NaCl, pH 7.0.

Figure 3

Complementary A–T, G–C and G–C^+ base-pairs in Watson–Crick, reversed Watson–Crick, Hoogsteen and reversed Hoogsteen pairing schemes. Possible base pairs for the modified nucleotide 1-deaza-adenine are shown.

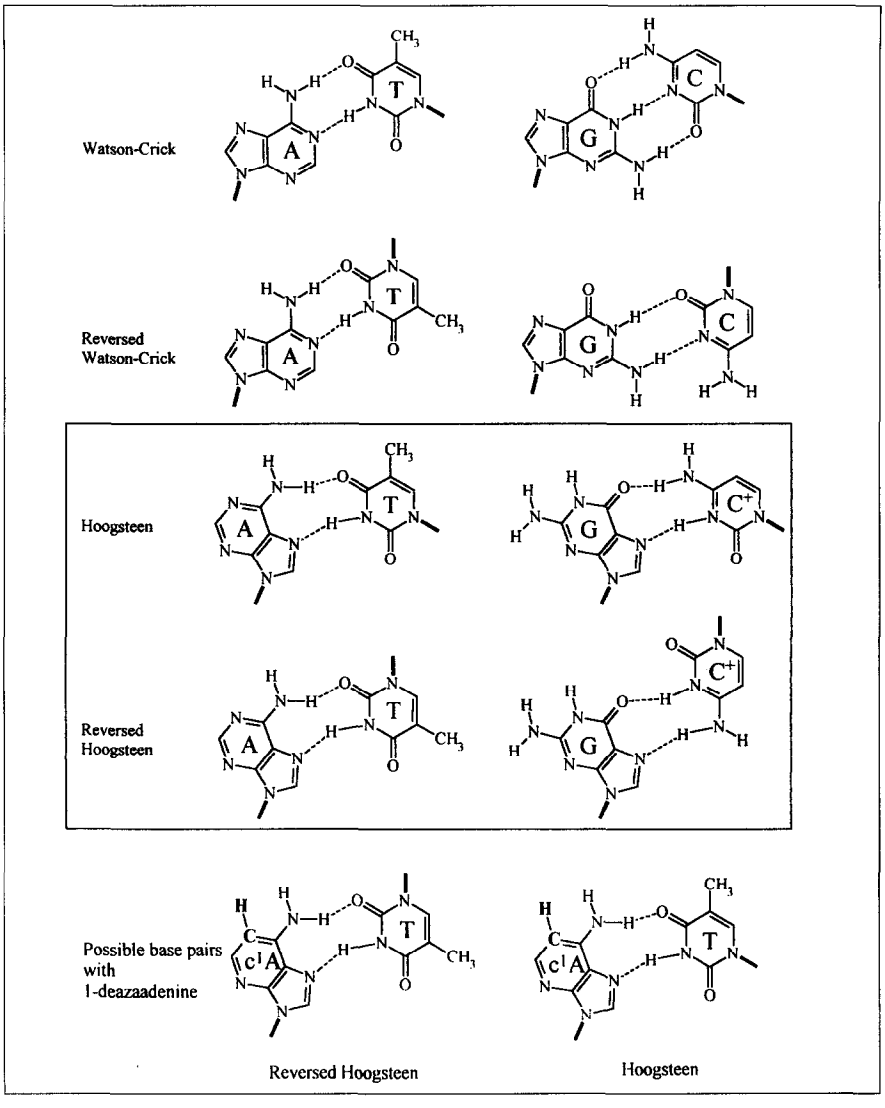

temperature, and the T-decamer bound to the Hoogsteen side of the purine strand dissociates at higher temperature. The differences in the CD spectra associated with the different stages of the triple helix denaturation in the two systems investigated (Fig. 4b) also support this idea. Inspection of the bands near 210 nm clearly shows that the melting of the Hoogsteen strand in the natural triplex is associated with a large increase in ellipticity. In the natural system this increase is observed for the transition at lower temperature, whereas in the bicyclic system it is observed for the higher temperature transition.

Bicyclo-DNA sequences containing 1-deazaadenine

We next investigated the UV-melting profile of a duplex consisting of bcd(T_{10}) and a bcd(A_{10}) strand in which the central bicyclodeoxyadenosine nucleotide was replaced by bicyclodeoxy-1-deazaadenosine (c^1A). This modification would give a mismatch in the Watson–Crick base-pairing scheme, but gives a match for either Hoogsteen or reversed Hoogsteen pairing (Fig. 3).

The synthesis of the corresponding phosphoramidite building block **7** was analogous to that for the natural ribo-series [27], and started from the bicyclic sugar analog **1** and the nitrobase **2** (Fig. 5). Lewis-acid-promoted nucleosidation afforded an anomeric mixture of the nitronucleoside **3**, which was subsequently reduced to the amino derivative **4**. Benzoylation of the amino group in compound **4**, followed by hydrolysis of the ester functions, yielded compound **5**, which was then converted into the trityl derivative **6**, the two anomeric forms of which could be separated by chromatography. The phosphoramidite **7** was subsequently

Figure 4

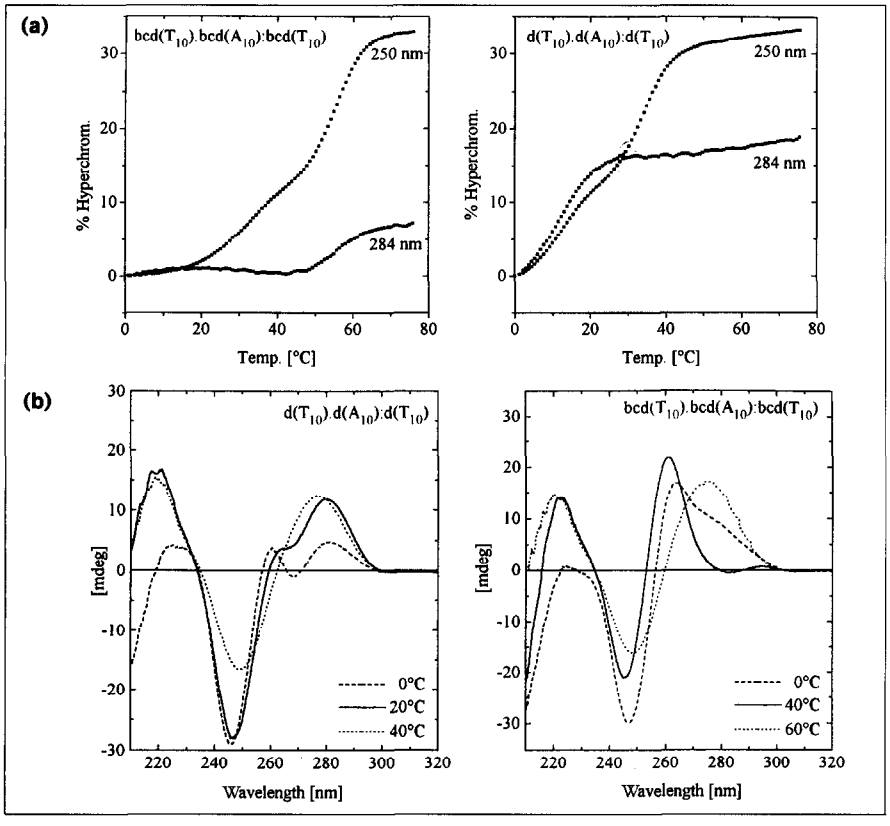

Triplex formation in bicyclo-DNA shows more stable Hoogsteen pairing, and less stable Watson–Crick pairing, than natural DNA. **(a)** UV-melting curves and **(b)** temperature dependent CD spectra of the natural and bicyclic T.A:T decamer triplexes (at a concentration of 2–3 μM in 10 mM NaH_2PO_4, 1M NaCl, pH 7.0).

obtained by standard procedures and used for the automated synthesis of the oligonucleotide sequence bcd($A_5(c^1A)A_4$), according to protocols previously described [25].

Figure 2 shows the UV-melting analysis of the duplex bcd($A_5(c^1A)A_4$).bcd(T_{10}), which revealed a T_m only 4° lower than that of the parent duplex (Table 1). This duplex is thus far more stable than those containing

Figure 5

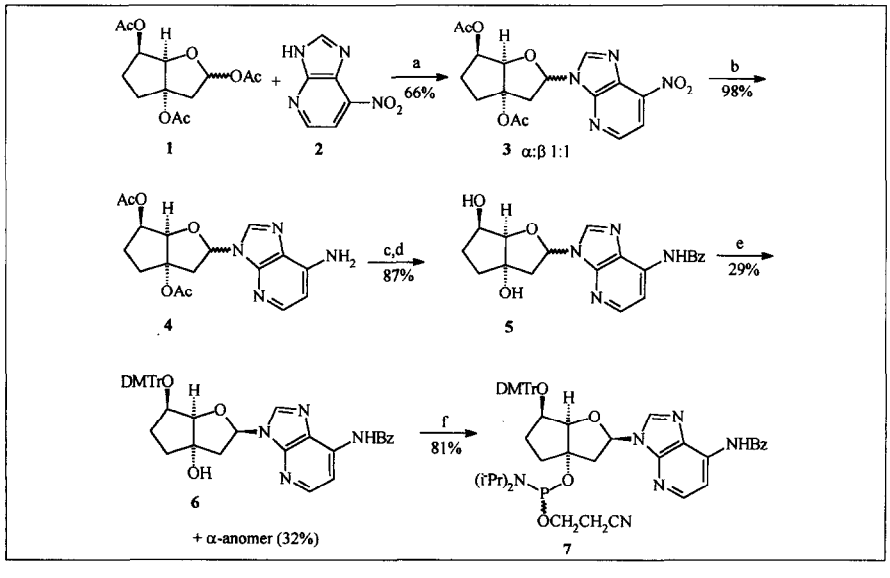

Synthesis of the nucleotide building block **7**, containing 1-deazaadenine. The following conditions were used for the transformations: a) CH_3CN, N,O-*bis*-trimethylsilylacetamide, $SnCl_4$, 45 °C, 4 h.; b) Pd/C (10 %), CH_3OH, room temperature, 5 bar, 7 h; c) BzCl, pyridine, 0 °C, 2 h; d) 0.2 M NaOH in $THF/CH_3OH/H_2O$ 5:4:1, 0 °C, 30 min.; e) $(MeO)_2Tr^+CF_3SO_3^-$, pyridine, room temperature, 3 h; f) $(NCCH_2CH_2O)(iPr_2N)PCl$, $iPrNEt_2$, THF, room temperature, 1 h.

an A–A or T–T mismatch (ΔT_m = 24-27°).This clearly demonstrates that, unlike natural DNA, bicyclo-DNA sequences use Hoogsteen or reversed Hoogsteen A–T pairing or both for duplex formation.

Bicyclo-DNA sequences containing all four nucleobases

To confirm that the preference for Hoogsteen-type duplex formation is directed by the sugar-phosphate backbone, and is not only a feature of oligo(A)–oligo(T) sequences, we investigated the pairing of the asymmetric purine sequence bcd(GGAAGGGAG) with its parallel- and antiparallel-oriented bicyclo-DNA complements at acidic pH. Assuming that the base orientation relative to the sugar is *anti* (the preferred arrangement in the mononucleosides), this sequence is expected to form Hoogsteen duplexes with isomorphous G–C$^+$ and A–T base-pairs with its parallel complement, whereas it is expected to form reversed Hoogsteen base pairs with non-isomorphous G–C$^+$ and A–T base-pairs with the antiparallel complement (Fig. 3). UV-melting curves in both cases exhibit highly cooperative transitions with increasing T_m at decreasing pH, as expected for G–C$^+$ base-pair formation (Fig. 6; Table 2, H,I). In all cases dominant self association of either the purine strand or the pyrimidine strand could be excluded (Fig. 6a, traces c and d).

Table 2

T_m values as a function of pH.

	Sequence	pH 5.0	5.5	6.0	6.5	7.0	8.0
H	bcd(GGAAGGGAG)/ bcd(CCTTCCCTC)	56 6	51.9	45.1	36.0	24.9	16.7
I	bcd(GGAAGGGAG)/ bcd(CTCCCTTCC)	56.1	47.5	38.6	28.2	16.4 30.5	– 31.1
J	bcd(GGAAGGGAG)/ bcd(CCTACCCTC)	16.9					
K	bcd(GGAAGGGAG)/ bcd(CTCCCATCC)	14.5					

Values are shown for the antiparallel and parallel complementary duplexes H, I as well as the antiparallel and parallel complementary duplexes J, K containing one A–A mismatch. Conditions were: λ = 260 nm, concentrations 4–6μM in 10 mM NaH_2PO_4, 1 M NaCl.

In the parallel system the dependence of T_m on pH (Fig 6a, inset) in the interval of pH 5.0–8.0 is non-linear, with increasing T_m at decreasing pH. The pK_a of the cytosine bases in the duplex appears to be well above that measured for the mononucleoside cytidine [28]. This strongly correlates with observations in the natural DNA series [29]. CD-spectroscopic analysis (Fig. 7) of the duplex, as expected, shows its structure to be quite

Figure 6

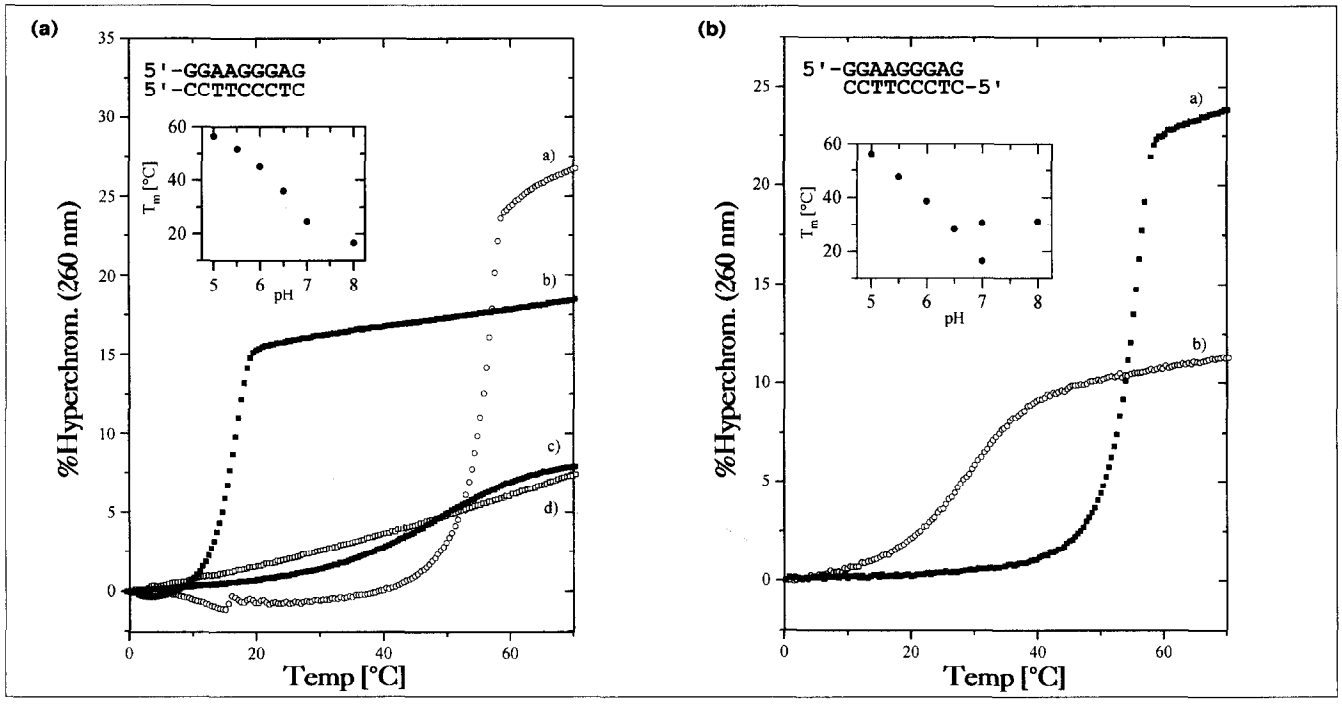

G/C-containing, bicyclo-DNA strands form Hoogsteen type duplexes **(a)** UV melting curves of the parallel Hoogsteen duplex H at pH 5.0 (trace a) and 8.0 (trace b) as well as of the separate pyrimidine (trace c) and purine (trace d) strands, both at pH 5.0. Inset: pH vs T_m profile for the duplex between pH 5.0 and 8.0. Conditions as in Table 2.

(b) UV melting curves of the antiparallel duplex I, exhibiting reversed Hoogsteen pairing at pH 5.0 (trace a) and Watson–Crick pairing at pH 8.0 (trace b). Inset: pH vs T_m profile for the duplex between pH 5.0 and 8.0. Conditions as in Table 2.

Figure 7

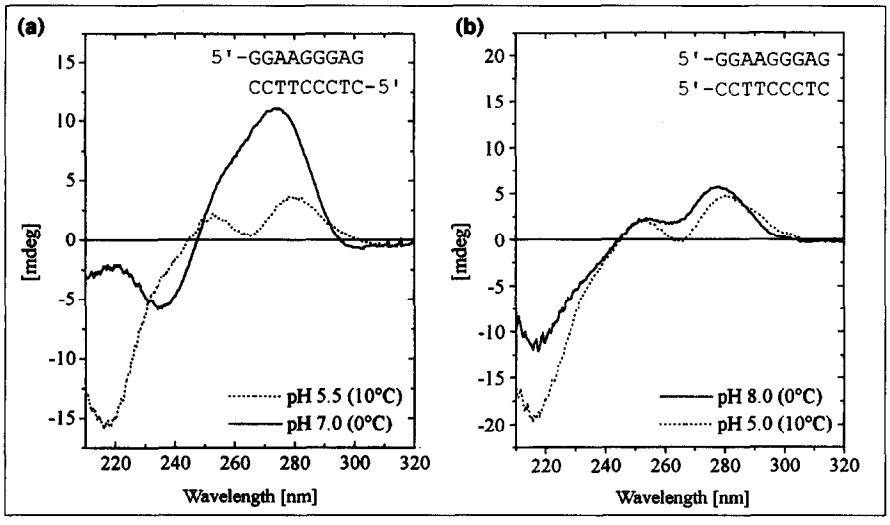

Base-pairing preferences of bicyclo-DNA are pH dependent. The CD spectra of the **(a)** antiparallel and **(b)** parallel oriented duplexes at varying pH values are shown. Conditions as in Table 2.

different from that of Watson–Crick and reversed Watson–Crick duplexes but very similar to that recently reported for a designed Hoogsteen duplex of natural DNA [5]. This observation underlines the strong tendency of bicyclo-DNA to prefer the Hoogsteen association mode with isomorphic A–T and G–C$^+$ base-pairs.

A similar analysis of the antiparallel complementary system bcd(GGAAGGGAG)/ bcd(CTCCCTTCC) shows melting curves with different hyperchromicity at low and high pH, indicating that the duplex structures under these conditions are different (Fig. 6b). In this system the melting temperatures are invariant in the pH range 7.0–8.0 but increase with decreasing pH in the range of pH 7.0–5.0. The CD spectra of the duplex at pH 8.0 and 5.5 (Fig. 7) are very different from each other, the former indicating an antiparallel Watson–Crick duplex at high pH, the latter bearing similarities to that of the parallel duplex at the same pH. The low-pH CD spectrum can only be ascribed to an antiparallel duplex exhibiting reversed Hoogsteen A–T and G–C$^+$ base-pairs. At pH 7.0 a biphasic melting event is observed, indicating that the antiparallel Watson–Crick and the reversed-Hoogsteen duplexes exist in equilibrium at this pH.

Parallel Hoogsteen and antiparallel reversed Hoogsteen duplex formation are both base selective, as can be seen from stability measurements of duplexes containing an A–A mismatch near to the center of the sequence. In both cases a drastic reduction of T_m relative to the matched sequence is observed (Table 2, J,K). In contrast to the Hoogsteen type of association, antiparallel strand alignment is strongly favored over a parallel orientation when Watson–Crick base pairs are formed. Under low salt conditions (0.15 M NaCl), the antiparallel Watson–Crick duplex bcd(GGATGGGAG).bcd(CTCCCATCC) exhibits a T_m value of 18.1 °C, but no cooperative melting is observed for the system that consists of the same purine-rich strand and a pyrimidine-rich strand with the opposite chain orientation [30].

Computer modeling

We have modeled the Hoogsteen duplex with parallel chain orientation (Table 2, H) to obtain insight into the main structural features of this pairing system. After a dynamics simulation on a 200 ps trajectory, a right-handed helical structure emerged, with all bases paired and in stacking distance from each other except for the two 5'-terminal nucleotides (Fig. 8). The conformation of the sugar-phosphate backbone stabilizes with torsion angles α,γ,δ and ε *trans*-oriented, and β and ζ either *+gauche*, *+gauche* or *trans*, *–gauche* oriented (Fig 9). The most significant structural differences relative to B-DNA are therefore in torsion angles α and γ, the former giving rise to a *trans*-phosphodiester conformation. All torsions generally correspond to ground-state conformations, as expected given the observed stability of this double helix.

Significance

The correlation of the sugar-phosphate backbone structure of DNA with its base-pairing properties is a challenging problem in supramolecular chemistry. DNA analogs that have defined and localized structural changes relative to natural DNA are excellent tools to rationalize such structure–activity relationships. The repetitive unit of 'bicyclo-DNA' deviates from that of natural B-DNA only by a shift of backbone torsion angle γ from the synclinal to the antiparallel range. Given this structural constraint, the alternative Hoogsteen and reversed Hoogsteen binding modes become strongly favored over the normal Watson–Crick mode. This is fundamentally different

Figure 8

Modeled structure of a parallel-chain Hoogsteen duplex. A stereo view of the average for the last 10 structures from a 200 ps dynamics simulation of the Hoogsteen duplex H (Table 2) is shown. Pyrimidine strand in yellow, purine strand in red, solvent omitted.

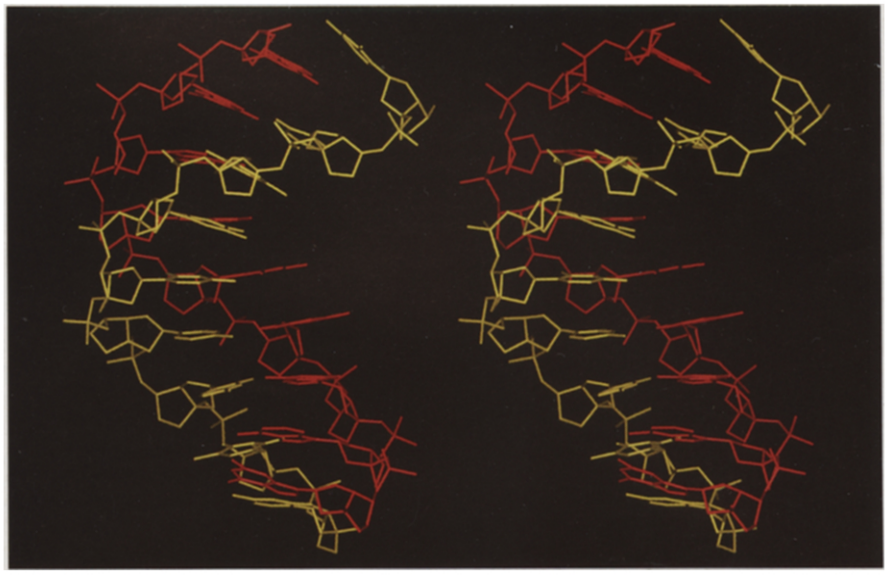

from the behavior of natural DNA, where even duplexes designed to bind in the Hoogsteen mode prefer to disproportionate to triple-helical structures with matched Hoogsteen and mismatched Watson–Crick strands [31]. Base pairing in bicyclo-DNA is degenerate with respect to strand polarity, so that Hoogsteen and reversed Hoogsteen paired structures are almost equally stable, despite the lack of

Figure 9

Two possible orientations for the sugar-phosphate backbone of bicyclo-DNA emerge from computer modeling. Detailed stereoviews of the two possible repeating backbone units, with torsion angles β and ζ, **(a)** *+sc*, *+sc* and **(b)** *ap*, *−sc*, respectively, are shown. *sc*, syclinal; *ap*, antiperiplanar.

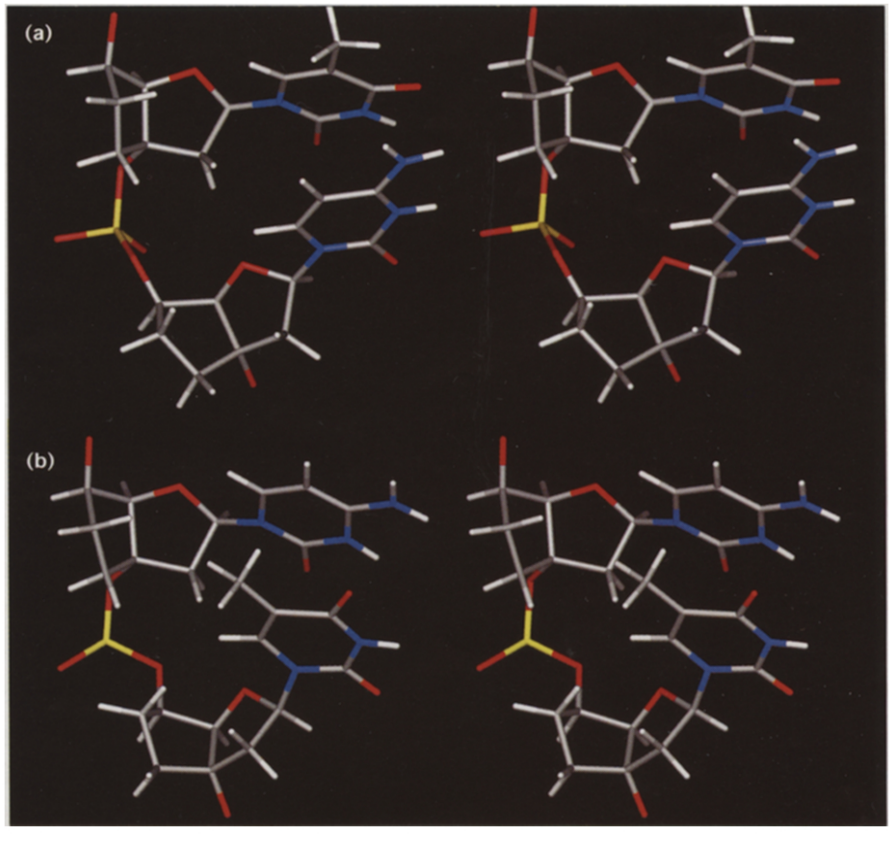

isomorphism of reversed Hoogsteen base pairs. In bicyclo-DNA, Watson–Crick duplexes are only stable if they contain G–C base pairs. In strand lengths up to decamers, no stable Watson–Crick duplex containing only A–T pairs has been identified.

The orientation of torsion angle γ seen in bicyclo-DNA is, in principle, accessible for natural DNA and has been observed in the repeating dinucleotide backbone unit of Z-DNA (in G nucleotides), in DNA–intercalator complexes (see, for example, [32]) and in the intertwined C–C$^+$ duplex tetrad (the i-motif), but has not been reported for DNA structures with a regular mononucleotide backbone unit. The study of DNA analogs such as this one should contribute to the understanding of DNA and RNA structure and association. The existence of nucleic acid analogs that add a discrimination between association modes to the normal base-pair selectivity may also further increase the selectivity of DNA and RNA recognition.

Materials and methods

*Synthesis of the monomeric compounds **3–7***

The synthesis of the 1-deazaadenine containing the bicyclodeoxynucleoside building block **7** was performed as outlined in Figure 5 using standard laboratory procedures. For general conditions see [22,25]. Compounds **3–6** were characterized by infrared spectroscopy (IR), UV/VIS spectroscopy (UV), ^{1}H- and ^{13}C-NMR and mass spectrometry (MS).

*Preparation of phosphoramidite **7***

To a solution of the trityl derivative **6** (144 mg, 0.21 mmol) in dry THF (2.5 ml) were added under Ar at room temperature $(iPr)_2NEt$ (145 µl, 0.85 mmol) and $(NCCH_2CH_2O)(iPr)_2NPCl$ (94µ, 0.42 mmol). After stirring for 1 h at room temperature, the mixture was diluted with AcOEt (15 ml) and extracted with saturated $NaHCO_3$ (2 x 10 ml). The organic phase was filtered, concentrated *in vacuo* and the residue purified by column chromatography (SiO_2, hexane/AcOEt) to give the phosphoramidite **7** (151 mg, 81 %) as a 1:1 mixture of diastereoisomers (^{1}H-NMR) in form of a white foam. Data of **7**: TLC (hexane/AcOEt 1:4): R_f 0.69/0.72; IR(CCl_4): 3419w, 3066w, 3037w, 2969m, 2934m, 2874w, 2836w, 2256w, 1695m, 1618s, 1588m, 1509s, 1493w, 1470s, 1447w, 1397m, 1365m, 1320m, 1312m, 1280m, 1250s, 1200m, 1180s, 1157m, 1126m, 1041s, 1002m, 978m, 968m, 896w, 877w, 837m, 700m; ^{1}H-NMR (300 MHz, $CDCl_3$): 1.09–1.19 (m, 12H, 2 $CH(CH_3)_2$); 1.47–1.71, 1.77–2.11 (m, 4H, H-C(6'), H-C(7')); 2.20–2.37, 2.53–2.67, 3.09–3.21 (3m, 4H, H-C(2'), OCH_2CH_2CN); 3.49–3.74 (m, 4H, $CH(CH_3)_2$, OCH_2CH_2CN); 3.76 (s, 6H, OCH_3); 3.84–3.94 (m, 2H, H-C(4'), H-C(5')); 6.48 (dt, J = 9.2, J = 5.2, 1H, H-C(1')); 6.73–6.88 (m, 4H, H_{ar}); 7.14–7.30 (m, 2H, H_{ar}); 7.35–7.45 (m, 4H, H_{ar}); 7.46–7.63 (m, 5H, H_{ar}); 8.02 (d, J = 7.0, 2H, H_{ar}); 8.36 (2s, 2H, H-C(2), H-C(1)); 8.44 (s, 1H, H-C(8)); 9.23 (s,br, 1H, HN). ^{31}P-NMR (400 MHz, d_6-benzene, ext. standard PPh_3 = 0 ppm): 159.3, 159.8.

Synthesis of oligomers

All oligo-bicyclodeoxynucleotides were prepared on solid phase on a DNA synthesizer (Pharmacia LKB Gene Assembler Special) using phosphoramidite methodology. The syntheses were performed on 0.8–1.5 µmol scales according to the protocol adapted for oligo-bicyclodeoxynucleotides described earlier [25] and proceeded with coupling yields ranging from 85 % (c^{1}A)-nucleotide to >97 % (A,T,C,G-nucleotides). After standard removal of protecting groups (trityl off mode) and detachment from the solid support (25 % NH_3, 55 °C, 12–16 h), oligomers were purified to homogeneity by DEAE ion-exchange high pressure liquid chromatography (hplc), and their sequence integrity was analyzed by matrix-assisted laser desorption-ionization time-of-flight mass spectrometry as described in [33] (Table 3). All experimentally determined molecular masses $(M-H)^-$ were found to be within 1.5 % of the calculated mass.

UV-melting curves

A Varian Cary 3E UV/VIS-spectrometer equipped with a temperature controller unit and connected to a Compaq ProLinea 3/25 zs personal computer was used. Temperature gradients of 0.5 ° min^{-1}. were applied and data points were collected in intervals of ~0.3°. % Hyperchrom. (wavelength) = 100 x $((D(T)-D_o)/D_o)$; D(T), absorption at temperature T; D_o, lowest absorption in the temperature interval. The transition temperature T_m was determined as described [34]. Extinction

Table 3

Synthesis and analytical data of oligo-bicyclodeoxynucleotides.

Sequence[a]	Scale (µmol)	HPLC[b]	Isolated yield OD(260 nm) [%]	MALDI-TOF-MS $[M-H]^-$ m/z (calc.)	m/z (found)
bcd(ATATATATAT)	0.8	30–40% B in 30 min; t_R 22.5 min.	30.7 (45)	3285.4	3286.2
bcd(AAAAA(c^{1}A)AAAA)	1.3	40–75% B in 30 min; t_R 16 min.	15.1 (11)	3328.5	3328.7
bcd(AAAAATAAAA)	0.8	28–42% B in 42 min; t_R 28 min.	34.6 (46)	3320.5	3321.7
bcd(TTTTTATTTT)	1.3	20–40% B in 30 min; t_R 25.5 min.	57.7 (55)	3248.4	3249.3
bcd(TTTTATTTTT)	1.3	20–40% B in 30 min; t_R 24.5 min.	66.6 (64)	3248.4	3251.0
bcd(GGAAGGGAG)	1.5	25–45% B in 30 min (60°C); t_R 19 min.	56.0 (47)	3086.3	3090.9
bcd(CCTTCCCTC)	1.0	30–40% B in 30 min; t_R 10.4 min.	26.5 (47)	2819.1	2820.3
bcd(CTCCCTTCC)	1.3	30–40% B in 30 min; t_R 21 min.	36.2 (51)	2819.1	2822.3
bcd(CTCCCATCC)	1.1	42–52% B in 30 min; t_R 13 min.	19.6 (30)	2828.1	2829.0
bcd(CCTACCCTC)	1.5	30–45% • in 30 min; t_R 21 min.	69.7 (78)	2828.1	2833.2

[a]The sequences bcd(A_{10}) and bcd(T_{10}) were previously characterized [25]
[b]Nucleogen DEAE 60-7, 125 x 4.0 mm (Macherey & Nagel); A = 20 mM KH_2PO_4 in H_2O:MeCN 4:1, pH 6.0; B = A + 1 M KCl; flow: 1 ml min^{-1}; detection wavelength: 260 nm.

coefficients of oligonucleotides were experimentally determined as described in [35].

CD-spectroscopy

CD-spectra were recorded on a Jasco J-500A spectropolarimeter with IF-500 II Interface connected to an PC/AT personal computer. The cell was thermostated by a Julabo F20 circulating bath. Temperatures were determined directly in the sample solution.

Molecular modeling

The duplex H was built using canonical B-DNA torsion angles and known Hoogsteen hydrogen bonding distances and geometry. The C(3')–C(5') ethylene bridge was then introduced to the natural DNA nucleotides. The nucleobases were fixed and the backbone torsion angles α, β, ϵ and ζ restrained to values of −46°, −147°, 155° and −96° resp., while the endocyclic torsion angles γ and δ in the newly constructed bicyclic sugar system were relaxed *in vacuo* by Polak–Ribière conjugate gradient (PRCG) minimization to a gradient <0.1 kJ Å^{-1}. All the calculations were carried out as implemented by the esff forcefield of Biosym/Molecular Simulations' Discover 95.0 package on a Silicon Graphics Indigo 2 workstation. All restraints were then removed and a 5 Å sphere of water (440 molecules) was placed around the duplex. Sixteen random solvent molecules were replaced by Na^+ to obtain overall charge neutrality. The non-bonded coulombic electrostatic cutoff was extended to 20.0 Å and a distance dependent dielectric constant of 1.0 was used. The solvated duplex was then subjected to PRCG minimisation to a gradient of <0.05 kJ Å^{-1} mol^{-1} followed by 200 ps of dynamics at 298.0 K. (1.5 fs timestep). The velocities were recorded every 1.0 ps throughout the simulation.

Supplementary material available

Synthesis details for compounds **3–6** and the result of a 200 ps dynamics simulation of the Watson–Crick duplex.

Acknowledgements

We thank the Swiss National Science Foundation (Grant 20-42107.94), Ciba-Geigy AG, Basel, the Ciba Jubiläumsstiftung and the Wander Stiftung, Bern for financial support.

References

1. Wang, A.H.-J., *et al.*, & Rich, A. (1979). Molecular structure of a left-handed double-helical DNA fragment at atomic resolution. *Nature* **282**, 680–686.
2. van de Sande, J.H., *et al.*, & Jovin, T.M. (1988). Parallel-stranded DNA. *Science* **241**, 551–557.
3. Germann, M.W., Kalisch, B.W. & van de Sande, J.H. (1988). Relative stability of parallel- and antiparallel-stranded duplex DNA. *Biochemistry* **27**, 8302–8306.
4. Ramsing, N.B. & Jovin, T.M. (1988). Parallel-stranded duplex DNA. *Nucleic Acids Res.* **16**, 6659–6676.
5. Liu, K., Miles, H.T. & Sasisekharan, V. (1993). A novel DNA duplex. A parallel-stranded DNA helix with Hoogsteen base pairing. *Biochemistry* **32**, 11802–11809.
6. Raghunatan, G., Miles, H.T. & Sasisekharan, V. (1994). Parallel nucleic acid helices with Hoogsteen base pairing: symmetry and structure. *Biopolymers* **34**, 1573–1581.
7. Beal, P.A. & Dervan, P.B. (1991). Second structural motif for recognition of DNA by oligonucleotide directed triple-helix formation. *Science* **251**, 1360–1363.
8. Moser, H.E. & Dervan, P.B. (1987). Sequence specific cleavage of double helical DNA by triple helix formation. *Science* **238**, 645–650.
9. François, J., Saison-Behmoaras, T. & Hélène, C. (1988). Sequence-specific recognition of the major groove of DNA by oligodeoxy-nucleotides via triple helix formation. Footprinting studies. *Nucleic Acids Res.* **16**, 11431–11440.
10. Cooney, M., Czernuszewicz, G., Postel, E.H., Flint S.J. & Hogan, M.E. (1988). Site-specific oligonucleotide binding represses transcription of the human c-myc gene *in vitro*. *Science* **241**, 456–459.
11. Gehring, K., Leroy, J. & Guéron, M. (1993). A tetrameric DNA structure with protonated cytosine.cytosine base pairs. *Nature* **363**, 561–565.
12. Chen, L., Cai, L., Zhang, X. & Rich, A. (1994). Crystal structure of a four-stranded intercalated DNA: d(C_4). *Biochemistry* **33**, 13540–13546.
13. Kang, C., Zhang, X., Ratliff, R., Moyzis, R. & Rich, A. (1992). Crystal structure of four-stranded *Oxytricha* telomeric DNA. *Nature* **356**, 126–131.
14. Smith, F.W. & Feigon, J. (1992). Quadruplex structure of *Oxytricha* telomeric DNA oligonucleotides. *Nature* **356**, 164–168.
15. Laughlan, G., *et al.*, & Luisi, B. (1994). The high-resolution crystal structure of a parallel-stranded guanine tetraplex. *Science* **265**, 520–524.
16. Böhringer, M., *et al.*, & Eschenmoser, A. (1992). Why pentose and not hexose nucleic acids? Part II, preparation of oligonucleotides containing 2',3'-dideoxy-β-D-glucopyranosyl building blocks. *Helv. Chim. Acta* **75**, 1416–1477.
17. Hunziker, J., *et al.*, & Eschenmoser A. (1993). Why pentose and not hexose nucleic acids? Part III, Oligo,2',3'-dideoxy-β-D-glucopyranosyl)-nucleotides (Homo-DNA): base pairing properties. *Helv. Chim. Acta* **76**, 259–352.
18. Otting, G., Billeter, M., Wüthrich, K., Roth, H.-J., Leumann, C. & Eschenmoser, A. (1993). Why pentose and not hexose nucleic acids? Part IV, 'Homo-DNA': ^{1}H-,^{13}C-,^{31}P- and ^{15}N NMR spektroscopic investigation of ddGlc (A-A-A-A-A-T-T-T-T-T) in aqueous solution. *Helv. Chim. Acta* **76**, 2701–2756.
19. Eschenmoser, A. & Dobler, M. (1992). Why pentose and not hexose nucleic acids? Part I. Introduction to the problem, conformational analysis of oligonucleotide single strands containing 2',3'-dideoxyglucopyranosyl building blocks ('Homo-DNA'), and reflections on the conformation of A- and B-DNA. *Helv. Chim. Acta* **75**, 218–259.
20. Pitsch, S., Wendeborn, S., Jaun, B. & Eschenmoser, A. (1993). Why pentose- and not hexose-nucleic acids? Part VII. Pyranosyl-RNA ('p-RNA'). *Helv. Chim. Acta* **76**, 2161–2183.
21. Pitsch, S., *et al.*, & Eschenmoser A. (1995). Pyranosyl-RNA ('p-RNA'): base-pairing selectivity and potential to replicate. *Helv. Chim. Acta* **78**, 1621–1635.
22. Tarköy, M., Bolli, M., Schweizer, B. & Leumann, C. (1993). Nucleic acid analogues with constraint conformational flexibility in the sugar phosphate backbone (bicyclo-DNA). Part I, Preparation of (3'S,5'R)-2'-deoxy-3',5'-ethano-α,β-D-ribofuranosyl-nucleosides (Bicyclonucleosides). *Helv. Chim. Acta* **76**, 481–510.
23. Egli, M., Lubini, P., Bolli, M., Dobler, M. & Leumann, C. (1993). Crystal structure of a parallel duplex of a deoxycytidyl-(3'-5')-deoxycytidine analogue containing intranucleosidyl C(3')-C(5') ethylene bridges. *J. Am. Chem. Soc.* **115**, 5855–5856.
24. Tarköy, M. & Leumann, C. (1993). Synthesis and pairing properties of decanucleotides from (3'S,5'R)-2'-deoxy-3',5'-ethano-β-D-ribo-furanosyladenine and -thymine. *Angew. Chem. Int. Ed. Engl.* **32**, 1432–1434.
25. Tarköy, M., Bolli, M. & Leumann, C. (1994). Nucleic acid analogues with restricted conformational flexibility in the sugar phosphate backbone (bicyclo-DNA). Part 3, Synthesis, pairing properties and calorimetric determination of duplex and triplex stability of decanucleotides from (3'S,5'R)-2-Deoxy-3',5'-ethano-β-D-ribo-furanosyladenine and thymine. *Helv. Chim. Acta* **77**, 716–744.
26. Pilch, D.S., Levenson, C. & Shafer, R.H. (1990). Structural analysis of the $(dA)_{10}.2(dT)_{10}$ triple helix. *Proc. Natl. Acad. Sci. USA* **87**, 1942–1946.
27. Cristalli, G., Franchetti, P., Grifantini, M., Vittori, S., Bordoni, T. & Geroni, C. (1987). Improved synthesis and antitumor activity of 1-deazaadenosine. *J. Med. Chem.* **30**, 1686–1688.
28. Saenger W. (1984). Physical properties of nucleotides: charge densities, pK values, spectra, and tautomerism. In *Principles of Nucleic Acid Structure*, p. 105–115. Springer-Verlag, New York.
29. Lavelle, L. & Fresco, J.R. (1995). UV spectroscopic identification and thermodynamic analysis of protonated third strand deoxycytidine residues at neutrality in the triplex d(C^+–T)$_6$:[d(A–G)$_6$.d(C–T)$_6$]; evidence for a proton switch. *Nucleic Acids Res.* **23**, 2692–2705.
30. Hunziker J. & Leumann C. (1995). Nucleic acid analogues: synthesis and properties. In *Modern Synthetic Methods*. (Ernst, B. & Leumann, C. eds), pp. 331–417, Verlag Helvetica Chimica Acta, Basel.
31. Bhaumik, S.R., Chary, K.V.R., Govil, G., Liu, K. & Miles, H.T. (1995). NMR characterization of a triple stranded complex formed by homo-purine and homo-pyrimidine DNA strands at 1:1 molar ratio and acidic pH. *Nucleic Acids Res.* **23**, 4116–4121.
32. Egli, M., Williams, L.D., Frederick, C.A. & Rich, A. (1991). DNA–nogalamycin interactions. *Biochemistry* **30**, 1364–1372.

33. Pieles, U., Zürcher, W., Schär, M. & Moser, H.E. (1993). Matrix-assisted laser desorption ionization time-of-flight mass spectrometry: a powerful tool for the mass and sequence analysis of natural and modified oligonucleotides. *Nucleic Acids Res.* **21**, 3191–3196.
34. Marky, L.A. & Breslauer, K.J. (1987). Calculating thermodynamic data for transitions of any molecularity from equilibrium melting curves. *Biopolymers* **26**, 1601–1620.
35. Bolli, M., Lubini, P. & Leumann, C. (1995). Nucleic acid analogs with restricted conformational flexibility in the sugar-phosphate backbone ('bicyclo-DNA'). Part 5, synthesis, characterization and pairing properties of oligo-α-D-(bicyclodeoxynucleotides) of the bases adenine and thymine (α-bicyclo-DNA). *Helv. Chim. Acta* **78**, 2077–2096.